AIAA JOURNAL
Vol. 36, No. 3, March 1998

Scaling Effects in Sublaminate-Level Scaled Composite Laminates

David P. Johnson*
Mississippi State University, Mississippi State, Mississippi 39762
John Morton†
Royal Aerospace Establishment, Farnborough, Hampshire GU14 6TD, England, United Kingdom
Sotiris Kellas‡
Lockheed Martin Engineering and Sciences Company, Inc., Hampton, Virginia 23681-0001
and
Karen Jackson§
U.S. Army Research Laboratory, Hampton, Virginia 23681-0001

A series of tensile tests has been performed to determine the effect of specimen size on the mechanical response of composite laminates that were scaled at the sublaminate level. The two material systems studied were AS4/3502 and APC-2. In the case of AS4/3502, three generic layups were considered: $[\pm 30/90_2]_{ns}$, $[\pm 45/0/90]_{ns}$, and $[90/0/90/0]_{ns}$ deg, where n = 1, 2, 3, or 4. For the APC-2 system, only the $[\pm 45/0/90]_{ns}$ deg layup was studied with n = 1 and 4. The effect of specimen size was examined with respect to first-ply failure strain, delamination onset strain, and ultimate stress and strain. In general, the strength of scaled specimens increased with increasing specimen size. Models from the literature were applied to attempt to explain the variations observed. It was found that the effect of ply constraint is not addressed properly in existing theories.

Introduction

SCALING effects can be defined as any deviation of the value of some mechanical property from an accepted law of mechanics. Some of the mechanical properties for which evidence of scaling effects were sought include stiffness, strength, strain at failure, first-ply failure, and the stress/strain response.

The importance of scale model testing has been demonstrated in areas such as aerodynamics and fluid mechanics, where data from scale model tests can be related to full-scale prototypes through well established laws. However, in structural design and, in particular, composite structures, there are no proven laws for predicting the structural response of full-scale components using scale model test data. Earlier research in the area of subscale testing[1–4] has indicated that complete similitude between a composite model and the full-scale component cannot be achieved. Factors such as the fiber diameter, resin rich regions, fiber/matrix interface, etc., cannot be scaled. Moreover, the laminated nature of fiber-reinforced composites adds another degree of complexity to the problem of scale model testing, due to the ply constraint, edge effects, multitude of damage modes, and method of scaling the stacking sequence. Two methods of varying the stacking sequence to increase the thickness of the laminate have been used. In the first method, the laminate thickness is increased by blocking several plies together, known as the ply-level scaling technique.[3] The second method, known as sublaminate-level scaling, employs the repetition of the basic sublaminate block n times to increase the thickness of the specimen, as shown in Fig. 1. From a similitude standpoint, ply-level scaling is the preferred method of scaling, because both the extensional and bending stiffness of scaled laminates remain unchanged with increased laminate thickness,[4] whereas with sublaminate-level scaling, only the extensional stiffness remains unchanged.

Received Jan. 14, 1997; revision received Oct. 29, 1997; accepted for publication Nov. 4, 1997.

*Assistant Professor, Department of Aerospace Engineering, M.S. 9549.
†Director, Structural Materials Centre, Defence Research Agency.
‡Principal Engineer, NASA Langley Research Center, Mail Stop 371, 144 Research Drive.
§Aerospace Engineer, Vehicle Technology Center, NASA Langley Research Center, Mail Stop 495. Associate Fellow AIAA.

A systematic study examining the effect of specimen size on the tensile response of several composite layups, employing ply-level scaling, has been presented by Kellas and Morton.[2] In agreement with the behavior of many brittle materials, a strength degradation was observed with increasing specimen size. The strength degradation with increasing specimen size was more pronounced in the matrix-dominated layups where off-axis plies carry a significant amount of the load. It is clear that the onset of damage, such as matrix cracking, depends on ply thickness.[5–13] Kellas and Morton[2] stated that this dependence on ply thickness was responsible for the observed strength trends. In a sublaminate-level scaling study,[3] it was found that the first-ply failure stress and the strength of $[\pm 45/\pm 45]_{ns}$ deg laminates increased significantly with increasing specimen size. The increase in strength was attributed to the diminishing effect of the two weak surface plies (where first-ply failures initiated) as the laminate thickness increased. First-ply failure initiated in the surface plies due to the reduced shear constraint that led to in-plane, normal-to-the-fiber stresses at the free edge.

As an extension to the earlier research on ply-level scaled laminates,[2] the present work was initiated to study three similar generic layups that have been scaled at the sublaminate level. Two carbon-fiber-reinforced composite systems were considered: AS4/3502 and APC-2, which consists of the same fiber (AS4) in a PEEK matrix. Three layup configurations using the graphite/epoxy material system were investigated. Because of limited resources, only one layup was investigated using the APC-2 system. A quasi-isotropic layup was chosen.

Experimental Details

Specimen Configuration

For the AS4/3502 material system, three generic layups were studied: $[\pm 30/90_2]_{ns}$, $[\pm 45/0/90]_{ns}$, and $[90/0/90/0]_{ns}$ deg, where $n = 1$, 2, 3, or 4. In the case of the APC-2 material system, only the $[\pm 45/0/90]_{ns}$ deg layup, where $n = 1$ and 4, was studied. The in-plane dimensions of the specimens were chosen to be $(12.5)n \times (125)n$ mm, labeled a, b, c, and d, where $n = 1$, 2, 3, and 4, respectively. Three techniques were used to scale the specimen dimensions (as seen in Fig. 2): one-dimensional scaling where in-plane dimensions were kept constant while the thickness was scaled, two-dimensional scaling where thickness was kept constant while the in-plane dimensions were scaled, and three-dimensional

Table 1 Test matrix

In-plane size	Specimen thickness			
	8 Ply	16 Ply	24 Ply	32 Ply
a	A B C D[a]	A B D	A B D	
b	A B C D	A B D		C
c			A B D	
d				A B C D

[a]A = $[\pm 30/90/90]_{ns}$, B = AS4/3502$[\pm 45/0/90]_{ns}$, C = APC-2 $[\pm 45/0/90]_{ns}$, and D = $[90/0/90/0]_{ns}$.

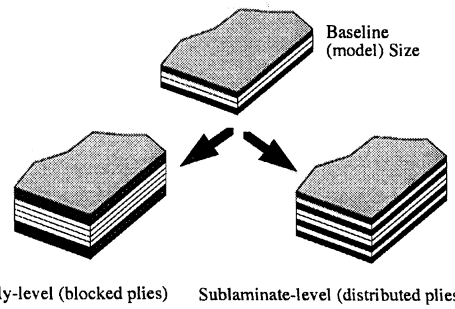

Fig. 1 Ply-level vs sublaminate-level scaling of laminate thickness.

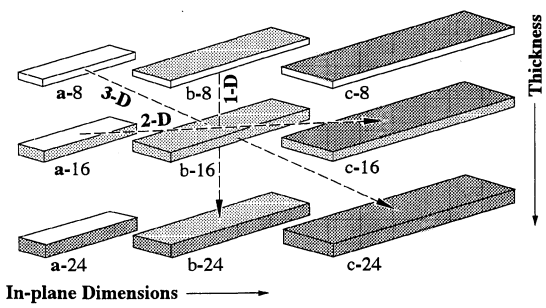

Fig. 2 In-plane and thickness scaling.

scaling where all three dimensions were scaled proportionally. The test matrix used in the present research is shown in Table 1.

Mechanical Testing

For each specimen size and laminate stacking sequence, at least five coupons were tested at a constant strain rate of approximately 3% strain/min until failure. The stress/strain response was then examined, and points of interest were identified. Such points of interest included the point at which the response became nonlinear, as well as any other recognizable kinks or knees in the response. The remaining specimens of each size were loaded to different proof loads, corresponding to these points of interest, and then removed from the test machine and examined for damage using nondestructive techniques. First-ply failure was detected using acoustic techniques, coupled with nondestructive examination. Longitudinal strain was recorded using a 25-mm gauge length extensometer.

Damage Examination

Two nondestructive damage examination techniques were employed to study the initiation and further development of damage in loaded specimens: dye penetrant-enhanced radiography and optical microscopy of polished specimen edges. The two techniques were used in conjunction to develop a three-dimensional assessment of the extent of damage at each load interval.

Presentation of Results

Results were obtained in the form of stress/strain plots, from which values of initial stiffness, ultimate stress, and strain at failure were extracted. Moreover, critical events, such as first-ply failure and delamination onset strain, were identified from the coupling of stress/strain response and nondestructive damage examination.

Epoxy-matrix specimens cut from the same panel showed consistent initial stiffnesses. However, the stiffnesses of specimens cut

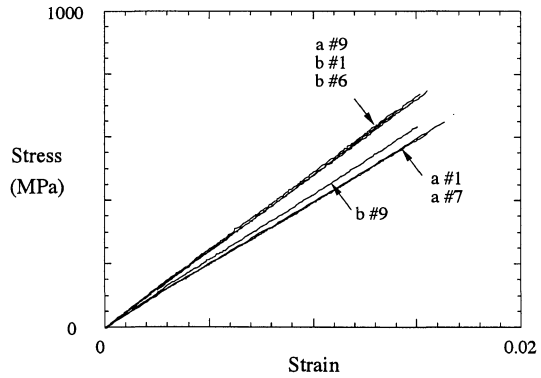

a) Response of eight-ply APC-2 $[\pm 45/0/90]_s$ specimens

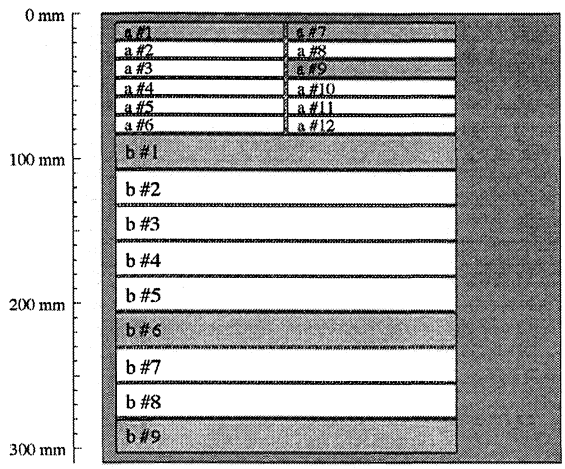

b) Position of specimens in the panel

Fig. 3 Stress/strain plots vs position in panel.

from different panels of the same layup but with scaled thickness did not necessarily coincide. To avoid this variation, resulting from inexact thickness scaling between different panels of a given layup, the average stress reported herein has been calculated using a nominal thickness. Hence, $\sigma_{av} = P/(nt_0w)$, where t_0 is the nominal thickness of an eight-ply specimen, w is the width of the actual specimen being examined, and n is the thickness scaling parameter. Justification for this assumption lies in the fact that the load-carrying capability of the laminate is governed by the fibers. Assuming negligible in-plane fiber migration during cure, which seems reasonable for the central portions of the panels, there are proportional numbers of fibers in scaled laminates, regardless of the actual thickness of the panels. The normalization process just described is nothing more than a normalization with respect to fiber volume fraction.

APC-2 specimens showed wide variations in stiffness for specimens cut from the same panel. Figure 3 shows the stress/strain plots of six representative specimens, all cut from the same eight-ply APC-2 $[\pm 45/0/90]_s$ deg panel, and the locations in the original panel from which they were cut. Specimens closest to the edge exhibited the lowest stiffness (and strength) values. Specimens cut more than 30 mm from the edge of the panel showed consistent stress/strain response. Thus, APC-2 strength and stiffness comparisons will be presented here only for specimens cut from the central portions of the panels.

Stress/Strain Response

One-dimensional and two-dimensional scalings were used, in addition to three-dimensional scaling (see Fig. 2), to identify which parameters most affected the mechanical response.

Three-Dimensional Scaled Specimens

Typical three-dimensional scaled stress/strain responses for all of the laminates studied are shown in Figs. 4–7. Scaling effects vary from quite pronounced to virtually insignificant, depending on the stacking sequence and matrix material.

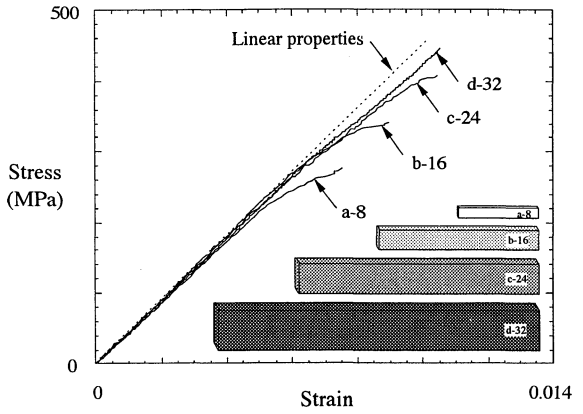

Fig. 4 Typical three-dimensional scaled response, $[\pm 30/90/90]_{ns}$.

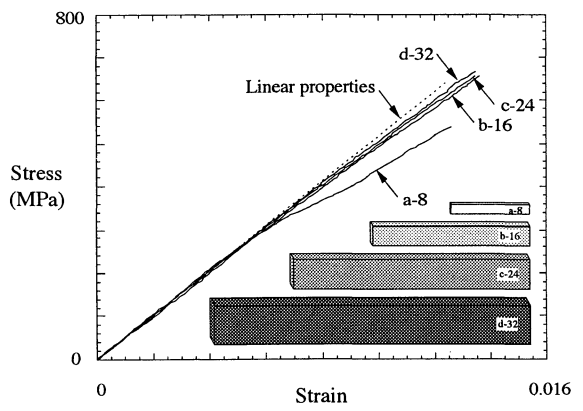

Fig. 5 Typical three-dimensional scaled response, AS4/3502 $[\pm 45/0/90]_{ns}$.

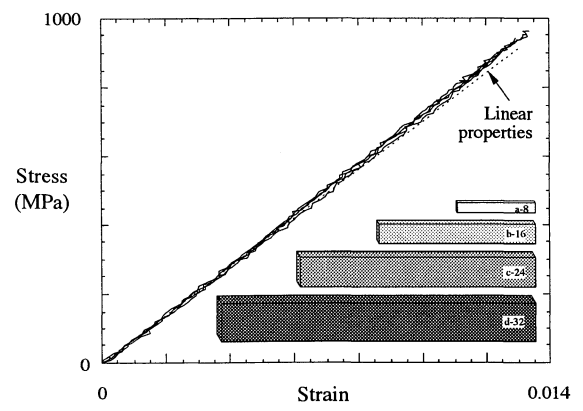

Fig. 6 Typical three-dimensional scaled response, $[90/0/90/0]_{ns}$.

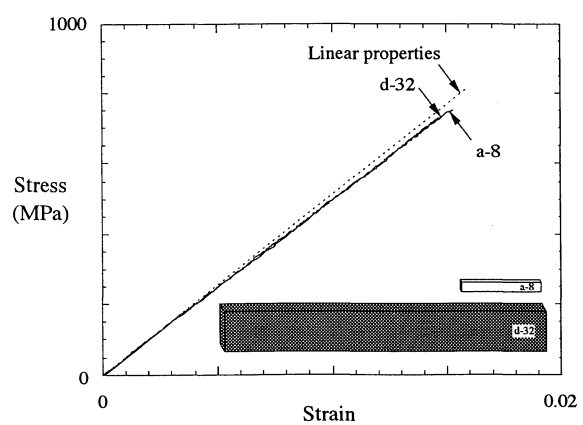

Fig. 7 Typical three-dimensional scaled response, APC-2 $[\pm 45/0/90]_{ns}$.

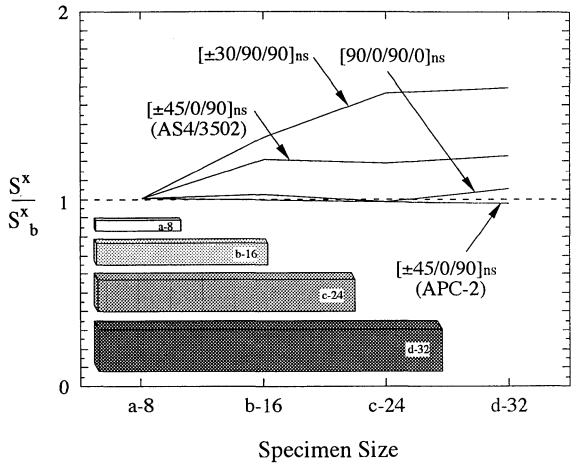

Fig. 8 Normalized strength of three-dimensional scaled specimens.

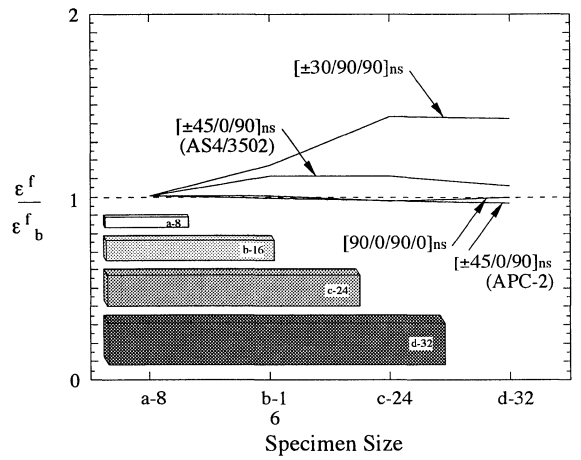

Fig. 9 Normalized ultimate strain of three-dimensional scaled specimens.

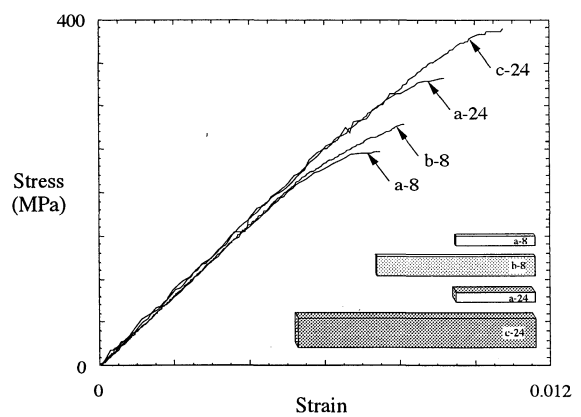

Fig. 10 Typical one-dimensional and two-dimensional scaled response, $[\pm 30/90/90]_{ns}$.

Normalized ultimate stress and strain for all layups studied are shown in Figs. 8 and 9. The specimens showing scaling effects in their stress/strain responses exhibited an increase in strength with larger specimen size. Only the $[\pm 30/90_2]_{ns}$ deg specimens showed significant increase in strain to failure.

One-Dimensional and Two-Dimensional Scaled Specimens

Typical stress/strain plots of $[\pm 30/90_2]_{ns}$ deg and epoxy-matrix $[\pm 45/0/90]_{ns}$ deg layups when using one-dimensional and two-dimensional scalings are shown in Figs. 10 and 11. Note that the stress/strain responses of the epoxy $[\pm 45/0/90]_{ns}$ deg specimens were virtually identical when the specimens' in-plane dimensions

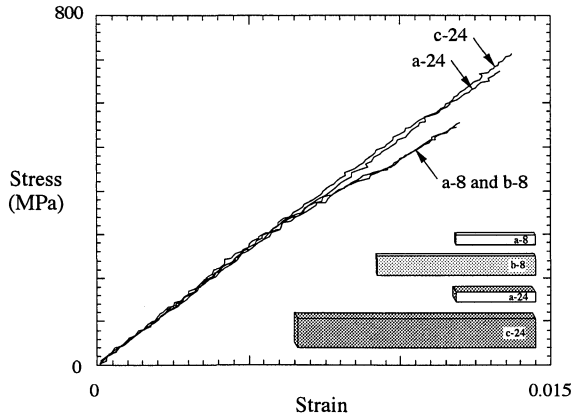

Fig. 11 Typical one-dimensional and two-dimensional scaled response, $[\pm 45/0/90]_{ns}$.

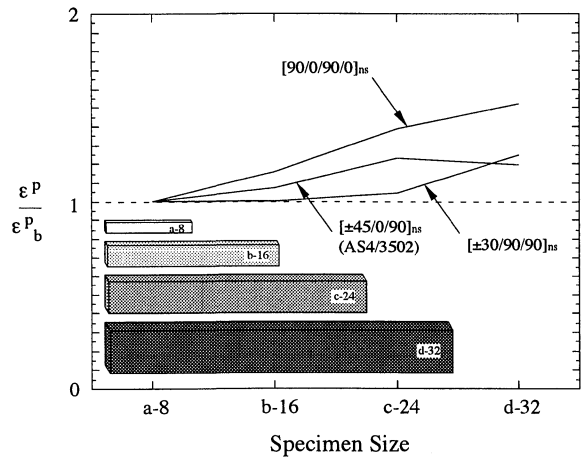

Fig. 12 Normalized first-ply failure strain of three-dimensional scaled specimens.

were varied (two-dimensional scaling), but when the thickness was varied (one-dimensional scaling) there was a pronounced change in the character and shape of the stress/strain curve analogous to the behavior noted using three-dimensional scaling.

Further, it is noted that the $[\pm 30/90_2]_{ns}$ deg specimens showed a similar tendency to about 80% of their ultimate strain, after which two-dimensional scaled specimens showed differing stress/strain responses. In particular, it appears that the smaller two-dimensional scaled specimens suffered premature or accelerated failures.

The fact that changes in specimen thickness lead to greater changes in mechanical response than changes in specimen in-plane dimensions indicates that the laminate thickness is the predominant scaled dimension, not the specimen volume, as is typically thought of when discussing brittle material scaling effects. However, there are some secondarily important effects in the in-plane (two-dimensional) scaling of $[\pm 30/90_2]_{ns}$ deg specimens.

Damage Evaluation

Normalized first-ply failure strain for all of the epoxy-matrix specimens is shown in Fig. 12. The crossply specimens showed the highest degree of dependence on specimen size, even though they did not show any significant variation in stress/strain response.

The data shown in Fig. 12 represent first-ply failure in single specimens, rather than averages of several. Hence, they are not statistically accurate, but general trends may still be observed.

In the case of the $[\pm 30/90_2]_{ns}$ and epoxy $[\pm 45/0/90]_{ns}$ deg specimens, a single specimen of each scaled size was loaded in the test machine until an audible crack was heard. The load was then reduced to zero, and the specimen was removed from the grips and x rayed. It was found that there was a one-to-one correspondence between the number of cracks heard before the load could be removed (usually 1–3) and the number of cracks appearing on the x rays.

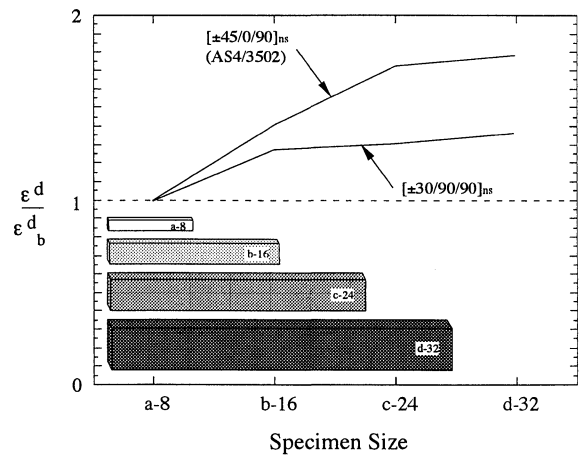

Fig. 13 Normalized delamination onset strain of three-dimensional scaled specimens.

First-ply failure in the $[90/0/90/0]_{ns}$ deg specimens could not be determined in this manner, as there were not any blocks of two or more 90-deg plies together in the laminate. Because the acoustic energy released from cracking of a single ply is smaller than for blocks of two or more plies, it is very difficult to resolve sounds from matrix cracks from other noises during the test. Hence, the first-ply failure strain was determined by loading several specimens to various proof loads and examining all of these specimens using the dye-penetrant x-ray technique. The values of the proof loads corresponded to intervals of strain approximately equal to 5% of the failure strain. The first specimen to manifest a crack in the x ray was used to record the first-ply failure strain.

Figure 13 shows normalized delamination onset strain for the $[\pm 30/90_2]_{ns}$ and epoxy $[\pm 45/0/90]_{ns}$ deg specimens. Both layups showed a marked increase in delamination strain with increased specimen size. These data were obtained in a manner similar to the detection of first-ply failure in the $[90/0/90/0]_{ns}$ deg specimens and corresponded to knees, or discontinuities, in the stress/strain plots.

$[\pm 30/90_2]_{ns}$ Degree Specimens

First-ply failure in $[\pm 30/90_2]_{ns}$ deg specimens occurred initially in the form of matrix cracks in the 90-deg plies. Specimens with 16 or more plies exhibited first-ply failure in the central block of four 90-deg plies. Cracks then appeared in the outermost (closest to the surface) block of two 90-deg plies, followed by cracks in all 90-deg plies. The outermost 90-deg cracks tended to occur at an angle, rather than normal to the applied load, indicating the presence of shear stresses, and were more closely spaced than the central 90-deg cracks. Figure 14 shows typical damage development in a 16-ply specimen. Point A on the stress/strain curve indicates first-ply failure, which occurs in the linear portion of the stress/strain response. The response diverges somewhat from linearity as the 90-deg ply cracking proceeds and before any other mode of failure occurs.

The next event in the development of damage in the $[\pm 30/90_2]_{ns}$ deg specimens was matrix cracking in the −30-deg plies adjacent to the centermost 90-deg cracks (point B on the stress/strain curve shown in Fig. 14). Some of the −30-deg cracking developed into local delaminations at the +30/−30 deg interfaces throughout the specimen thickness. However, the only general delamination that propagated along the edge was at the −30/90 and +30/−30 deg interfaces closest to the surface, peeling off the ±30-deg surface plies (point C on the stress/strain curve). With the propagation of this delamination, significant stiffness loss was noted, and in the smaller specimens (8- and 16-ply), global specimen failure quickly followed.

AS4/3502 $[\pm 45/0/90]_{ns}$ Degree Specimens

Damage in $[\pm 45/0/90]_{ns}$ deg specimens initiated in the form of matrix cracks in the central 90-deg block, followed by cracking in all 90-deg plies throughout the specimen thickness. Subsequently, delaminations initiated in the central 90-deg block, alternating from one 0/90 deg interface to the other. Typical damage development

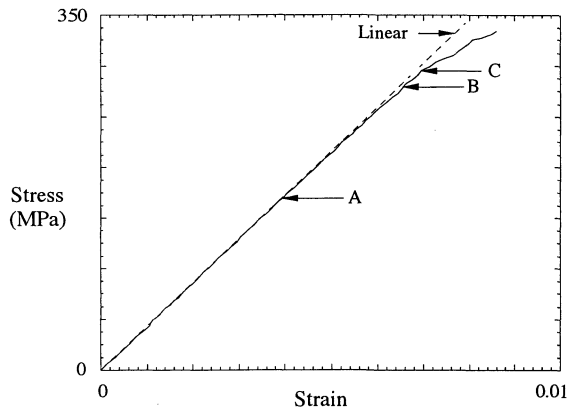

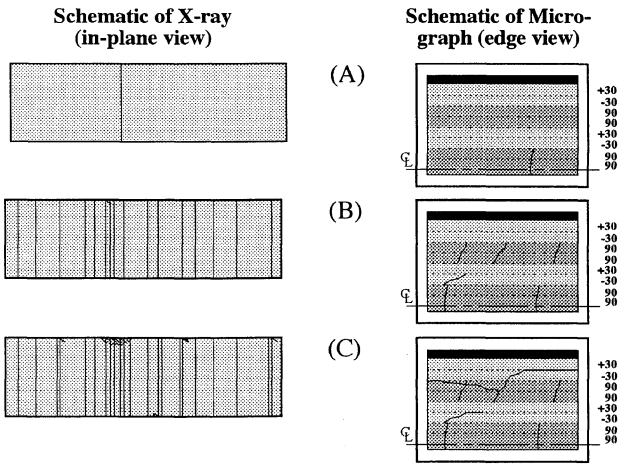

Fig. 14 Damage development, $[\pm 30/90/90]_{2s}$.

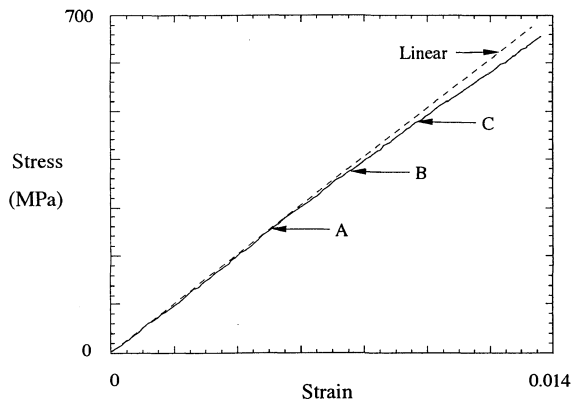

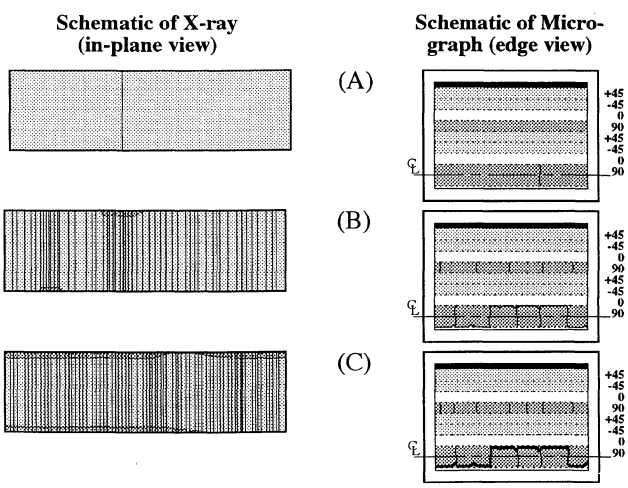

Fig. 15 Damage development, $[\pm 45/0/90]_{2s}$.

is correlated to the stress/strain response in Fig. 15 for a 16-ply specimen. It is evident that the first-ply failure (point A) has little effect on the stiffness. Not until the onset of delamination (point B) does the stiffness change appreciably. In eight-ply specimens, this delamination proceeded from the edge, inward toward the center of the specimen, until the coupon was virtually divided into two halves. Delaminations in larger specimens did not proceed to this extent before global failure, and the effect on stiffness was considerably less.

$[90/0/90/0]_{ns}$ Degree Specimens

The only damage observed prior to global failure in $[90/0/90/0]_{ns}$ deg specimens was matrix cracking in the 90-deg plies, which always initiated in the surface 90-deg plies. The small deviation from linear stress/strain response was actually strain stiffening, similar to that seen in unidirectional composites.

APC-2 $[\pm 45/0/90_2]_{ns}$ Degree Specimens

First-ply failure in PEEK-matrix $[\pm 45/0/90]_{ns}$ deg specimens consisted of matrix cracks in the 90-deg plies. Unlike the corresponding cracks in the epoxy-matrix specimens, cracks in the PEEK-matrix specimens did not run through the width of the coupon but were confined to the edges. The radiographs showed apparent cracks in the ±45-deg plies, as well as what appeared as edge delaminations along the full length of the gauge section. However, these regions along the specimen edges lacked the clearly defined edge typical of edge delaminations in epoxy-matrix specimens. Upon inspection of the polished edges of the specimens under the microscope, no evidence of either ±45-deg cracking or edge delamination was present. This damage on the radiographs may have been due to fiber/matrix debonding.

Discussion of Results

In contrast to the ply-level scaled results[2] and the volume scaling of brittle materials in general, such properties as the ultimate stress and strain, first-ply failure strain, and delamination onset strain, of the sublaminate-level scaled specimens in this study increased as n was scaled from 1 to 4. These differences result from changes in ply constraint when a specimen is scaled at the sublaminate level.

First-Ply Failure

It has been well documented that first-ply failures usually occur in the form of intralaminar cracks that may develop into delaminations depending on the stacking sequence and the ply thickness.[5] The relationship between intralaminar cracks and ply thickness has been researched for many years and it is generally accepted that well-constrained transverse plies will, in general, exhibit resistance to cracking. Although a number of semiempirical models are available, the strain prediction for the onset of cracking is rather poor, in the sense that trends can be predicted but not the actual critical strain levels. This was found to be particularly true for laminates containing thick blocks of 90-deg plies.[12]

General fracture mechanics principles can be used to show that, for instance, in $[90/0/90/0]_{ns}$ deg specimens, the initial failure will occur in the surface 90-deg plies rather than in the internal 90-deg plies, i.e., the stress concentration factor is higher for an edge crack than for an internal crack. But again, only general conclusions can be drawn, not specific predictions.

It can be shown that, for ply-level scaled specimens with the same ratio of 90 deg to constraining ply thicknesses, most of the energy-based models, e.g., Refs. 7, 8, 10, and 11, are reduced to Eq. (1). The subscripts s and b stand for scaled and baseline, respectively, and n is the scale factor:

$$\sigma_s^{cr}/\sigma_b^{cr} = 1/\sqrt{n} \tag{1}$$

Because the nonlinear stress/strain behavior in the laminates studied occurs well beyond the first-ply failure, Eq. (1) can be used for critical strain ε^{cr} as well, if thermal stresses are ignored.

Equation (1) suggests that the critical strain ratio for the onset of transverse cracking in two scaled specimens depends solely on n and is independent of layup. Consider, for example, the case of a $[\pm\theta_n/90_n]_s$ laminate. Given two values of n, Eq. (1) would predict the same critical strain ratio for all values of θ. This is physically

inaccurate because the stiffness of the constraining plies will, in reality, have an influence on the critical stress or strain ratio.

It has been shown that, in carbon fiber composites, the effect of thermal strains cannot be neglected because these can be of magnitudes comparable to the mechanical strains at failure.[7] Bailey et al.[7] used force equilibrium and strain compatibility to derive a simple expression for the thermally induced stress in a constrained 90-deg ply:

$$\sigma_{\text{th}} = \frac{\Delta T b^c E_2 E^c (\alpha^c - \alpha_2)}{E_2 t + E^c b^c} \tag{2}$$

where E^c, b^c, and α^c are the stiffness, thickness, and thermal expansion coefficient, respectively, of the constraining plies. The parameters E_2, t, and α_2 are the stiffness, thickness, and thermal expansion coefficient, respectively, of the 90-deg plies; and ΔT is the difference between operating and stress-free temperatures. This relationship is valid only if stresses in the direction of the 90-deg fibers are ignored, as per Ref. 8. Equation (2) predicts the same thermal stresses for all specimen sizes in a given family of laminates scaled using either ply-level or sublaminate-level scaling.

If Eq. (1) is used as a failure criterion, and thermal stresses are included along with mechanical stresses, it can be shown that larger specimens may exhibit matrix cracks due to thermal stresses alone, before mechanical strain is even applied. This is a well-known phenomenon with laminates with large numbers of plies blocked together and applies directly to ply-level scaled spiciness. It is not the case with sublaminate-level scaled specimens.

Whereas the consideration of the thermal stresses modifies Eq. (1) somewhat, the trend of increased first-ply failure strain in sublaminate-level scaled composites cannot be accounted for. Therefore, it is concluded that models that lead to Eq. (1), with or without thermal effects, are inadequate in their application to composite laminates.

Flaggs and Kural[8] used an energy-based model, developed by Parvizi et al.,[10] which can more readily be applied to sublaminate-level scaling. Their model, applied to scaled specimens with 90-deg surface plies, can be rewritten as

$$\frac{\varepsilon_s^{\text{cr}}}{\varepsilon_b^{\text{cr}}} = \left[\frac{b_s^c E_s^c (b_b^c E_b^c + t E_2)}{b_b^c E_b^c (b_s^c E_s^c + t E_2)} \right]^{\frac{1}{4}} \tag{3}$$

where b^c and E^c are the thickness and stiffness of the constraining plies, respectively; t is the thickness of the 90-deg ply; and E_2 is the longitudinal stiffness of the 90-deg ply. Subscripts s and b refer to scaled and baseline sizes, respectively. Thermal effects are neglected.

For the $[90/0/90/0]_{ns}$ specimens considered, using sublaminate-level scaling, Eq. (3) can be rewritten as

$$\frac{\varepsilon_s^{\text{cr}}}{\varepsilon_b^{\text{cr}}} = \frac{\sigma_s^{\text{cr}}}{\sigma_b^{\text{cr}}} = \left\{ \frac{1 + [E_2/6E_b^c]}{1 + [E_2/(8n-2)E_s^c]} \right\}^{\frac{1}{4}} \tag{4}$$

Using lamination theory, in conjunction with the elastic properties of AS4/3502, shown in Table 2, E^c was calculated for $n = 1, 2, 3$, and 4. Using these values, Eq. (4) predicted virtually no increase in first-ply failure strain. Clearly, the model is inadequate to explain the first-ply failure scaling effects shown in Fig. 12.

The discussion so far has revolved primarily around the issues concerning the initiation of damage in the scaled specimens. In general, the influence of first-ply failure on the subsequent response of the coupon is very slight, and the influence of subsequent matrix-related damage will depend on the stacking sequence and the matrix toughness. The role of the stacking sequence, so far as scaling effects are concerned, is demonstrated by the $[90/0/90/0]_{ns}$ specimens. Despite the significant scaling effects with respect to first-ply failure, shown in Fig. 12, the stress/strain response and the ultimate stress for these specimens were, in general, unaffected by scale size because of the presence of a significant number of 0-deg plies.

Table 2 Mechanical properties of AS4/3502

E_1	E_2	G_{12}	ν_{12}	α_1	α_2
136.9 MPa	9.86 MPa	5.65 MPa	0.29	−0.3*e*-6/°C	28.1*e*-6/°C

The role of matrix toughness is demonstrated by the PEEK-based specimens, which had the same fiber as the epoxy-based specimens but a tougher matrix. Because of the damage resistance of the matrix material, the delamination damage mode was entirely suppressed even in the smallest specimens, yielding a nearly linear stress/strain response and higher average stress at the point of fiber failure. Indeed, the PEEK matrix yielded an even higher fiber failure strain, which is typical of toughened matrix composites.

Delamination

In the present work, delamination had a profound effect on the stiffness and strength of $[\pm 30/90_2]_{ns}$ and $[\pm 45/0/90]_{ns}$ deg specimens. The effect of delamination on the strain at failure depended on the layup and, in particular, the presence of 0-deg plies. For example, $[\pm 45/0/90]_{ns}$ deg specimens showed essentially no scaling effect with respect to strain at failure, compared to $[\pm 30/90_2]_{ns}$ deg specimens (Fig. 9). Thus, whereas $[\pm 45/0/90]_{ns}$ deg specimens suffered a loss in stiffness due to delamination, the ultimate applied strain was controlled by the ultimate strain of the longitudinal fibers, which is relatively independent of specimen size. Hence, at the failure strain of the fibers, a delaminated specimen would support a lower average stress. This accounts for the strength scaling effect in $[\pm 45/0/90]_{ns}$ deg specimens because only the smallest (size a) specimens delaminated extensively.

Because they contained no 0-deg plies, scaling effects were most pronounced in the $[\pm 30/90_2]_{ns}$ deg specimens. A major contribution to the presence of scaling effects in this stacking sequence can be attributed to the observed damage mode. Because these specimens always delaminated at the outermost −30/90 and +30/−30 deg interfaces, the surface plies can be thought of as weak plies. The surface plies lose their capacity to carry load before global failure of the specimen. In the case of the smallest (size a-8) specimens, no other load-bearing plies remain, and global failure is precipitated by failure of the surface ±30-deg plies.

Size b-8 specimens (Fig. 10) exhibited failures at a higher applied stress because of the additional width of the specimen. The smaller in-plane dimensions of the a-8 specimens required little beyond delamination initiation to completely separate the specimen.

In the case of the larger sublaminate-level scaled specimens, increasingly more ±30-deg plies are available to redistribute the load. Therefore, as n increases, the effect of the weak surface plies becomes less important to the overall response of the specimen, and global strength increases.

Effects of laminate thickness on the onset of delamination were reported by, among others, O'Brien.[14,15] O'Brien derived a closed-form expression for the energy release rate G, as a function of the delamination onset strain ε^{cr}, the change in longitudinal modulus $(E - E^*)$, and the laminate thickness t_L. O'Brien's results can be expressed, for scaled laminates, as

$$\frac{\varepsilon_s^{\text{cr}}}{\varepsilon_b^{\text{cr}}} = \sqrt{\frac{E - E_b^*}{n(E - E_s^*)}} \tag{5}$$

In the case of specimens scaled at the ply level, Eq. (5) reduces to Eq. (1), as the stiffness loss term $(E - E^*)$ is identical regardless of ply-level scaled specimen size. In the case of sublaminate-level scaling, Eq. (5) predicts an increase in the delamination onset strain (Fig. 16), as the constraint term $(E - E^*)$ decreases sharply with increased scaled specimen size. Discrepancies between theory and experiment for the $[\pm 45/0/90]_{ns}$ deg specimens shown in Fig. 16 may be due to thermal stresses.

The performance of any model in predicting the mechanical behavior of a scaled composite structure using experimental data from a baseline specimen depends on the ability to predict the nature and location of damage. For example, the calculation of E^* requires prior knowledge of the delamination interfaces, as well as the state of the resulting sublaminates. In the case of specimens scaled at the ply level, information on the delamination sites can be provided by the baseline specimen. However, in specimens scaled at the sublaminate level, where the number of potential delamination sites for the baseline specimen is smaller than that of the scaled specimen, the delamination site of the scaled specimen has to be predicted using some interlaminar stress and/or energy consideration.

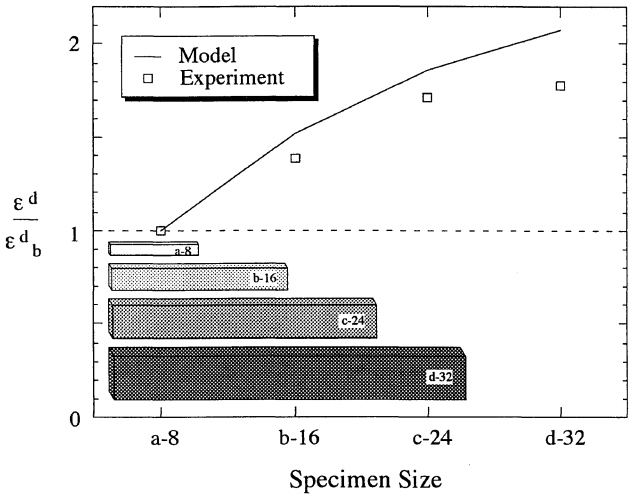

Fig. 16 Delamination onset strain data vs Eq. (5).

Concluding Remarks

The experimental results, both from the present work and earlier studies,[2,3] indicate that the strength scaling effect of epoxy-matrix specimens depends on the percentage of load-carrying plies that are in the laminate and on the damage modes occurring in the laminate. In general, the strength and strain to failure of fiber-dominated layups, not exhibiting delamination, are relatively independent of the specimen size in the range of sizes studied ($n = 1$–4), damage development, and method of scaling (ply or sublaminate level). This is evident, even though a 50% increase in first-ply failure strain was noted in $[90/0/90/0]_{ns}$ specimens.

On the contrary, the strength of matrix-dominated layups and fiber-dominated layups where delamination is present, depends on the specimen size, damage development, and the method of scaling. Whereas it has been shown that specimens scaled at the ply level exhibited strength degradation with increasing specimen size,[2,3] similar specimens scaled at the sublaminate level exhibited increased strengths with increasing specimen size. A strength increase of nearly 60% was recorded in the $[\pm 30/90_2]_{ns}$ deg specimens between the baseline and the full-scale specimens. The strength of the $[\pm 45/0/90]_{ns}$ deg specimens with 16 plies or more ($n \geq 2$) was approximately the same and at least 20% higher than that of the 8-ply specimens. In both cases, the strength appeared to be controlled by the nature and extent of damage prior to failure. Consequently, strength scaling models could be developed from simpler models currently used for the prediction of critical loads for the onset of matrix damage. Further study would be useful to investigate the ramifications these conclusions would have on fatigue loaded specimens. It is suspected that scaling effects would also be present in fatigue.

In the case of PEEK-matrix specimens, scaling effects were much less pronounced when compared to the corresponding epoxy-matrix specimens. In particular, there was no delamination in PEEK-matrix $[\pm 45/0/90]_{ns}$ deg specimens. However, scaling effects in PEEK-matrix specimens have been observed in $[\pm 45/\pm 45]_{ns}$ deg type specimens,[3] where significant plastic shear deformation was present in the matrix material. This indicates that, where matrix damage is limited, scaling effects are suppressed.

In the future, it would be useful to consider larger specimens, as full-size structures may be orders of magnitude larger than the specimens used to determine laminate properties. Even if there were a small scaling effect in, for example, the crossply specimens, the effect may become significant in very large structures.

Several models from published literature were applied with varying degrees of success to predict the first-ply failure and delamination stress in scaled composites. It was found that the effect of ply constraint is not addressed properly in the existing theories. This was particularly evident when some of the models were used to predict the relative change in the critical loads for the onset of matrix damage with specimen size.

Acknowledgments

This work was carried out with the support of the NASA Langley Research Center under Contract NAS1-187471. Thanks are due to the Contract Monitor, Huey D. Carden.

References

[1]Morton, J., "Scaling of Impact-Loaded Carbon-Fiber Composites," *AIAA Journal*, Vol. 26, No. 8, 1988, pp. 989–994.

[2]Kellas, S., and Morton, J., "Strength Scaling in Fiber Composites," *AIAA Journal*, Vol. 30, No. 4, 1992, pp. 1074–1080.

[3]Kellas, S., and Morton, J., "Damage and Failure Mechanisms in Scaled Angled-Ply Laminates," *Fourth Composites Symposium on Fatigue and Fracture*, edited by W. Stinchcomb, ASTM STP 1156, American Society for Testing and Materials, New York, 1993, pp. 257–280.

[4]Jackson, K. E., "Scaling Effects in the Static and Dynamic Response of Graphite-Epoxy Beam-Columns," NASA TM 102697, July 1990.

[5]Wang, A. S. D., "Fracture Mechanics of Sublaminate Cracks in Composite Materials," *Composites Technology Review*, Vol. 6, No. 2, 1984, pp. 45–62.

[6]Crossman, F. W., and Wang, A. S. D., "The Dependence of Transverse Cracking and Delamination on Ply Thickness in Graphite/Epoxy Laminates," *Damage in Composite Materials*, ASTM STP 836, American Society for Testing and Materials, New York, 1984, pp. 118–139.

[7]Bailey, J. E., Curtis, P. T., and Parvizi, A., "On the Transverse Cracking and Longitudinal Splitting Behaviour of Glass and Carbon Fibre Reinforced Epoxy Cross Ply Laminates and the Effect of Poisson and Thermally Generated Strain," *Proceedings of the Royal Society of London, A*, Vol. 366, 1979, pp. 599–623.

[8]Flaggs, D. L., and Kural, M. H., "Experimental Determination of the In Situ Transverse Lamina Strength in Graphite/Epoxy Laminates," *Journal of Composite Materials*, Vol. 16, March 1982, pp. 103–115.

[9]Flaggs, D. L., "Prediction of Tensile Matrix Failure in Composite Laminates," *Journal of Composite Materials*, Vol. 19, Jan. 1985, pp. 29–50.

[10]Parvizi, A., Garrett, K. W., and Bailey, J. E., "Constrained Cracking in Glass Fibre-Reinforced Epoxy Cross-Ply Laminates," *Journal of Material Sciences*, Vol. 13, 1978, pp. 195–201.

[11]Caslini, M., Zanotti, C., and O'Brien, T. K., "Study of Matrix Cracking and Delamination in Glass/Epoxy Laminates," *Journal of Composites Technology and Research*, Vol. 9, No. 4, 1987, pp. 121–130.

[12]Nairn, J. A., "Microcracking, Microcrack-Induced Delamination and Longitudinal Splitting of Advanced Composite Structures," NASA CR 4472, Nov. 1992.

[13]Lagace, P., Brewer, J., and Kassapoglou, C., "The Effect of Thickness on Interlaminar Stresses and Delamination in Straight-Edged Laminates," *Journal of Composites Technology and Research*, Vol. 9, No. 3, 1987, pp. 81–87.

[14]O'Brien, T. K., "Characterization of Delamination Onset and Growth in a Composite Laminate," *Damage in Composite Materials*, edited by K. L. Reifsnider, ASTM STP 775, American Society for Testing and Materials, New York, 1982, pp. 140–167.

[15]O'Brien, T. K., "Mixed-Mode Strain-Energy-Release Rate Effects on Edge Delamination of Composites," *Effect of Defects in Composite Materials*, ASTM STP 836, American Society for Testing and Materials, New York, 1984, pp. 125–142.

A. M. Waas
Associate Editor